Enhancement of Glass Ablation Rate During Micro-via Processing using Very Long Pulse 248-nm Excimer Laser for Semiconductor Interposer Packaging

Yasufumi Kawasuji*[1], Akira Suwa[1], Yasuhiro Adachi[1], Tomonari Tanaka[1], Kouji Kakizaki[1], and Masakazu Washio[2]

[1]*Gigaphoton Inc., 400 Yokokura-shinden, Oyama-shi, Tochigi 323-8558, Japan*
[2]*Waseda University, 3-4-1 Okubo, Shinjuku-ku, Tokyo 169-8558, Japan*

**Corresponding author's e-mail: yasufumi_kawasuji@gigaphoton.com*

Much research on improving the productivity of micro-via fabrication in glass using 248-nm excimer laser ablation has been performed for semiconductor interposer packaging. We previously reported that the ablation rate for glass using long excimer laser pulses (74 ns time-integrated square (TIS)) is 1.53 times higher than that for short pulses (32 ns TIS) under the same laser fluence conditions. Here, we report further enhancement of the ablation rate using a very long pulse width (130 ns TIS) excimer laser. The ablation rate for 500-µm-thick glass using this laser is about 2.17 times higher than that for a conventional short-pulse excimer laser. We also investigate the dependence of the relationship between the ablation rate and the laser irradiation energy ratio on the time since the beginning of the pulse, and we find that after 30 ns, the relationship becomes linear. This is consistent with our previous results for the glass micro-via fabrication mechanism.

DOI: 10.2961/jlmn.2024.01.2007
Keywords: glass, interposer, micro-via, long pulse, excimer laser, ablation

1. Introduction

Micro-via fabrication in glass has been studied for post-5G semiconductor interposer packaging. Glass is the most suitable material for high-frequency semiconductor packaging due to its low loss tangent, very low surface roughness and very high form stability [1]. However, glass substrates are still not used for semiconductor packaging due to the difficulty of micro-via fabrication. Glass is a very brittle material; therefore, it is very difficult to fabricate micro-vias without causing cracking [2-4].

There have been many reports on glass micro-via fabrication using picosecond or femtosecond short-pulse laser irradiation [5-8]. However, a reliable method that is suitable for industrial applications has not been developed for fabricating micro-vias with high aspect ratios (>50) in glass.

The thickness of the glass substrate should be at least several hundred micrometers due to handling restrictions for semiconductor packaging. However, to achieve full penetration of such a substrate using short-pulse picosecond or femtosecond lasers requires the use of multiple pulses. To date, studies on glass processing have focused mainly on the processing efficiency for a single pulse [5] or the ability to drill in a very thin glass-fiber core [6]. Although the micro-via fabrication in thick glass substrates using multiple femtosecond pulses and problem the formation of microcracks in the glass as a result of the stress wave generated by the femtosecond laser ablation has been reported [8].

We previously reported the successful fabrication of high-aspect-ratio, high-quality micro-vias in glass using a KrF excimer laser, despite the fact that nanosecond pulses were employed [9]. Using long laser pulses (74 ns time-integrated square (TIS)), the ablation rate was found to be 1.53 times higher than that for short pulses (32 ns TIS) under the same laser fluence conditions. Thus, it was expected that the ablation rate could be further increased by extending the laser pulse width. Here, we report the results for the ablation rate during glass micro-via fabrication using very long (130 ns TIS) excimer laser pulses.

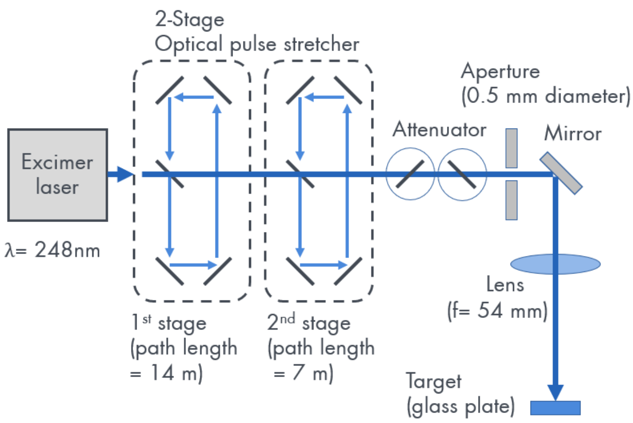

Fig. 1 Schematic diagram of laser ablation pulse width dependence test system.

2. Experimental setup

Figure 1 shows a schematic diagram of the test setup used for micro-drilling glass substrates with the KrF excimer laser. Table 1 shows the main output parameters for the excimer laser light source, Table 2 shows the experimental parameters, and Table 3 shows the specifications of the test sample.

A 2-stage optical pulse stretcher (OPS) is connected to an excimer laser light source (GT600K, Gigaphoton Inc.). The 1st stage of the OPS has a 14-m beam path, with a 47-ns optical propagation delay, and the 2nd stage has a 7-m beam path with a 23-ns optical propagation delay. The delayed beam then enters the attenuator and lens to irradiate the target surface at a set fluence.

Figure 1 also shows a diagram of the OPS. A laser beam irradiates a partially reflecting (60%) mirror, and the transmitted component is directly output. The reflected light component travels along the OPS beam path to create a propagation delay, and the delayed beam is then combined with the original beam path at the same partially reflecting mirror. The light is divided again by the mirror, and the transmitted light re-enters the OPS beam path and is re-propagated and combined with the beam path.

The pulse width for the OPS output can be discretely varied from 32 to 130 ns TIS by switching the partially reflecting mirror in the 1st and 2nd stage to a fully transparent window. This means that each OPS stage can be disabled individually. Table 4 shows the pulse width of the OPS output for different configurations of the 1st and 2nd stage entrance mirrors. Figure 2 shows the OPS output pulse waveform for each OPS configuration.
Here the pulse width is expressed as the TIS value. This is because the waveform for an excimer laser constitutes a pulse train as shown in Figure 2. Therefore, it is not suitable to use the full-width-at-half-maximum value.

The TIS value is given by

$$TIS = \frac{[\int I(t)\,dt]^2}{\int I(t)^2\,dt}$$

where I(t) is the intensity.

The waveform in Figure 2(a) is the same as that for an excimer laser light source, because both the 1st and 2nd stages of the OPS are disabled. The pulse width for the light source used in this experiment was 32.7 ns TIS. Figure 2(b) shows the waveform when the only 2nd stage of the OPS is enabled. It can be seen that the overall waveform is a combination of the original waveform and a 23-ns delayed waveform. Likewise, the waveform in Figure 2(c) is a combination of the original waveform and a 47-ns delayed waveform. Finally, Figure 2(d) shows a combination of the 47-ns and 23-ns delayed waveforms.

Figure 3 shows images of the glass surface laser irradiation profile for different OPS configurations, together with the irradiation beam diameter ($1/e^2$). The irradiation diameter is different for each OPS configuration due to variations of the beam propagation distance. It is therefore necessary to correct the irradiation energy based on the beam diameter to maintain a constant peak fluence. Table 5 shows the case where the peak fluence is maintained at 36.0 J/cm^2 by adjusting the attenuator.

Table 1 Main output parameters for Gigaphoton GT600K excimer laser light source used in this experiment.

Laser output parameter	Value
Wavelength [nm]	248
Pulse energy [mJ/pulse]	100
Repetition rate [Hz]	10-6000
Output laser power [W]	600
Pulse width TIS [ns]	32
Output beam size [mm]	7 x 20

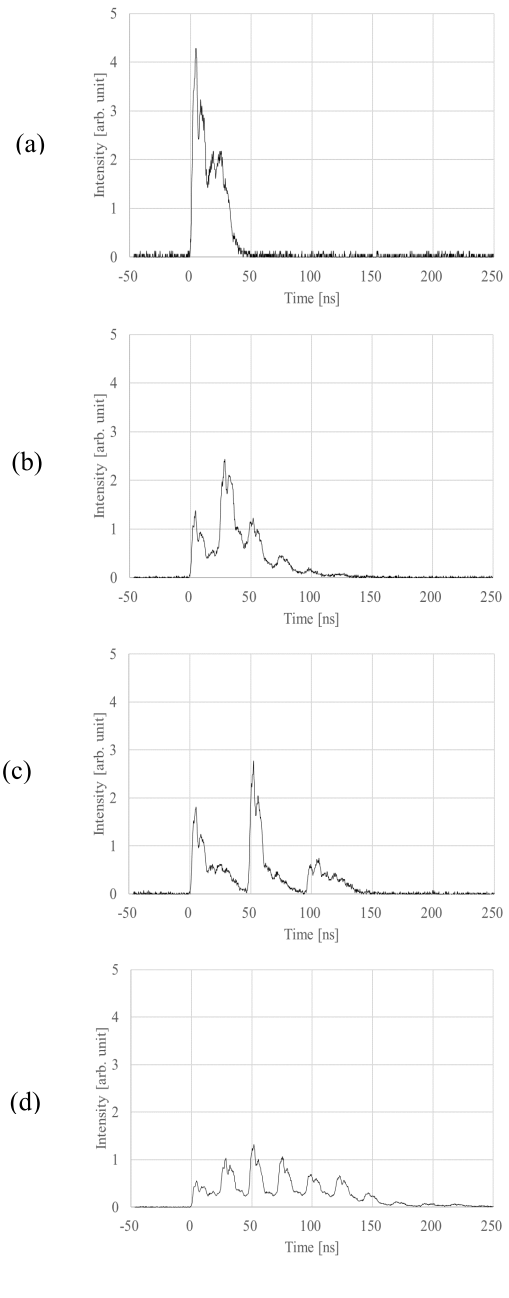

Fig. 2 Pulse waveform for 2nd stage OPS output of mirror for (a) configuration 1, (b) configuration 2, (c) configuration 3, and (d) configuration4.

Table 2 Experimental parameters.

Parameter	Value
Aperture diameter [mm]	0.5 (round shape)
Focal length of lens [mm]	54 (@248nm wavelength)

Table 3 Specifications of test sample

Parameter	Specification
Material	Non-alkali glass
Type	Eagle XG
Thickness [µm]	500
Manufacturer	Corning

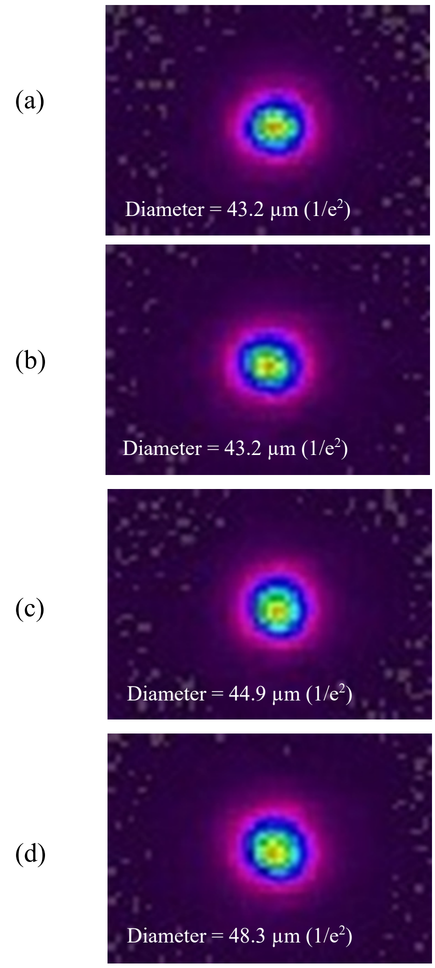

Fig. 3 Irradiation profile for (a) configuration 1, (b) configuration 2, (c) configuration 3, and (d) configuration4.

Table 4 OPS configuration and output pulse width.

OPS configuration	OPS1 entrance mirror	OPS2 entrance mirror	OPS output pulse width (ns TIS)
1	Fully transparent	Fully transparent	32.7
2	Fully transparent	Partially reflecting	65.6
3	Partially reflecting	Fully transparent	70.2
4	Partially reflecting	Partially reflecting	130.5

Table 5 Center peak fluence for each OPS configuration corrected by irradiation diameter.

OPS configuration	Irradiation diameter($1/e^2$, µm)	Radiation energy (mJ)	Peak fluence on glass surface (J/cm^2)
1	43.2	52.8	36.0
2	43.2	52.8	36.0
3	44.9	57.0	36.0
4	48.3	66.0	36.0

3. Experimental results

Figures 4 and 5 show the dependence of the ablation depth on the number of pulses for each OPS configuration. The target material was non-alkali glass (Eagle-XG, 500 µm thick, Corning Incorporated). The laser irradiation fluence was 36.0 J/cm^2. Table 6 shows the number of irradiation pulses required to penetrate the glass plate and the ablation rate enhancement ratio for the non-OPS condition. It can be seen that the penetration pulse reduction ratio increases by more than 2.17 times by increasing the pulse width from 32 to 130 ns TIS.

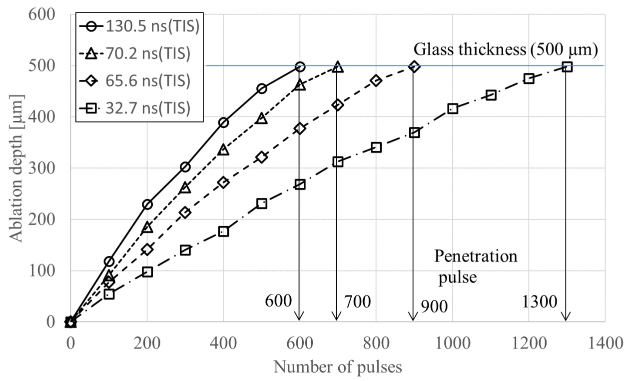

Fig. 4 Dependence of ablation depth on number of pulses for different pulse width conditions.

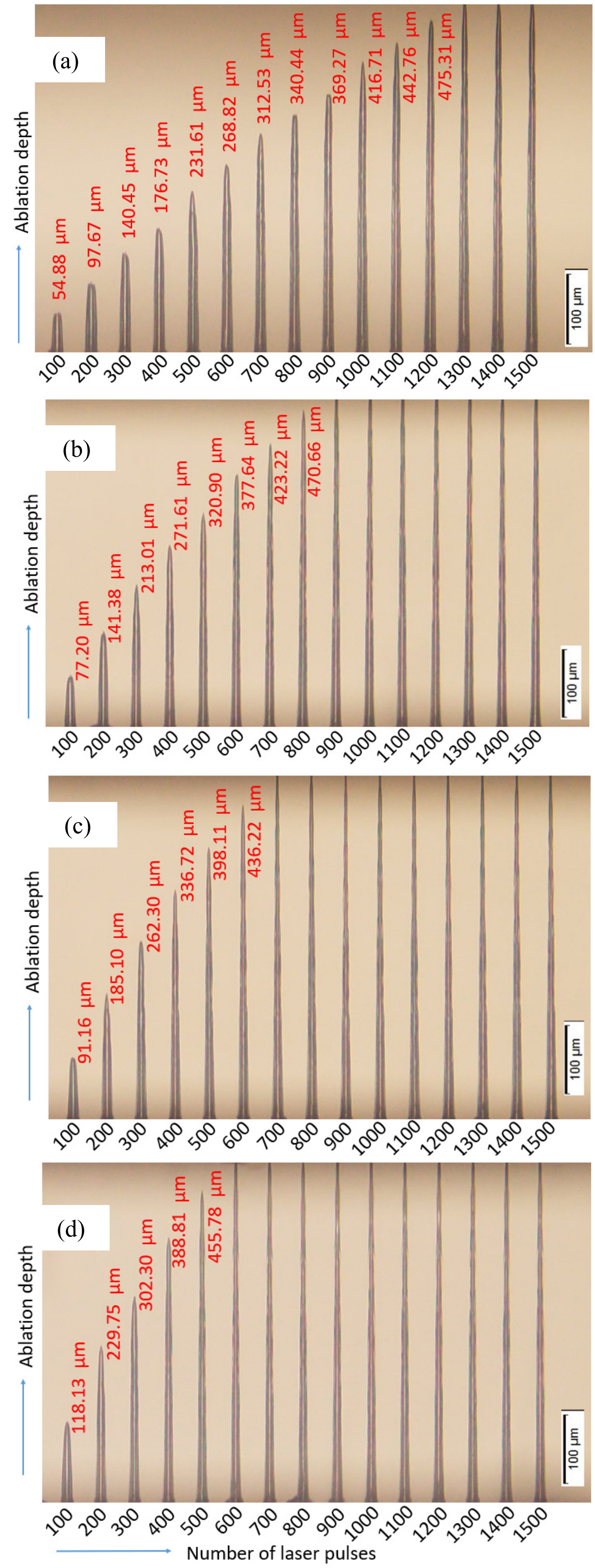

Fig. 5 Ablation depth for pulse widths of (a) 32.7 ns TIS, (b) 65.6 ns TIS, (c) 70.2 ns TIS, and (d) 130.5 ns TIS every 100 pulses from side of glass with central peak fluence of 36.0 J/cm2.

Table 6 Number of pulses required to penetrate glass plate.

Pulse width (ns)	Number of laser pulses needed to penetrate 500-µm-thick glass	Penetration pulse reduction ratio
32.7	1300	(1.00)
65.6	900	1.44
70.2	700	1.86
130.5	600	2.17

4. Discussion

In our previous research on time-resolved optical emission spectroscopy during glass ablation, we concluded that the laser energy after 30 ns determines the glass ablation rate [10]. To confirm this, we investigate the relationship between the ablation rate after 30 ns and the pulse energy ratio for the four OPS conditions.

Figures 6(a)-(d) show the pulse energy ratio after 30 ns for different OPS conditions. The red filled areas show the energy irradiated after 30 ns. The energy ratio for the entire pulse and the measured ablation depth after the first 10 pulses are shown in Table 7.

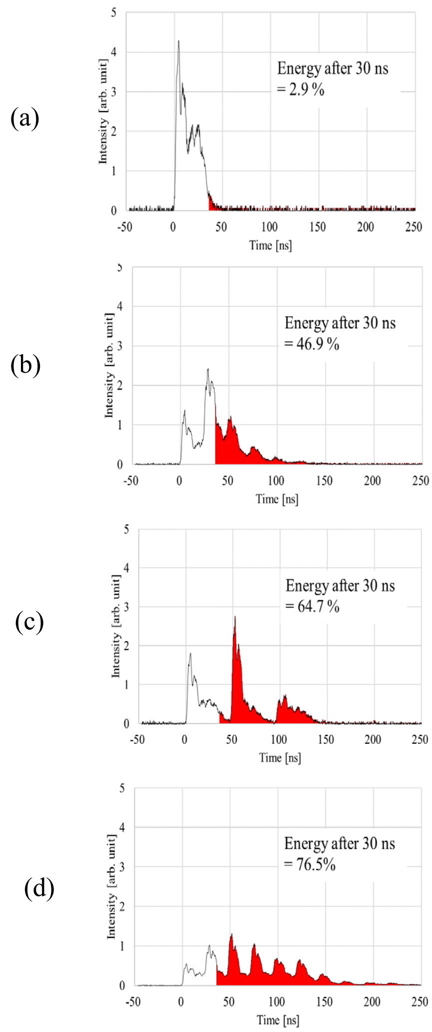

Fig. 6 Energy ratio after 30 ns, where red filled area shows energy after 30 ns for (a) configuration 1, (b) configuration 2, (c) configuration 3, and (d) configuration 4.

Table 7 Energy ratio after 30 ns and measured ablation depth after 10 pulses.

OPS configuration	Energy ratio after 30 ns (%)	Measured ablation depth of first 10 pulses (μm)
1	2.9	1.20
2	46.9	1.43
3	64.7	1.60
4	76.5	1.65

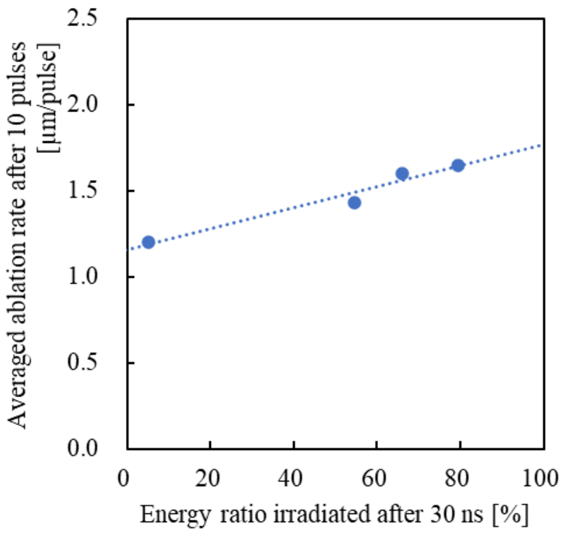

Fig. 7 Dependence of ablation rate averaged over 10 pulses on energy ratio after 30 ns.

The reason for using the ablation rate for the first 10 pulses is the nonlinear dependence of the ablation rate on the via depth for larger numbers of pulses, as shown in Figure 4. This nonlinearity may be the result of laser attenuation inside the vias. Also, the ablation depth was too small to accurately measure for less than 10 pulses.

Figure 7 shows the relationship between the average ablation rate for the first 10 pulses and the energy ratio after 30 ns. It can be seen that the relationship is linear.

5. Conclusion

It was found that by changing the excimer laser pulse width from 32 to 130 ns TIS, the processing rate could be more than doubled under the same fluence conditions. This confirms our previous proposal that the irradiated energy after 30 ns determines the ablation rate. A linear correlation was found between the ablation rate and the energy ratio after 30 ns for four different pulse widths of 32 to 130 ns.

The method proposed in the present study increases micro-via fabrication efficiency by more than two times, which not only leads to increased light utilization efficiency and downsizing of the micro-via fabrication equipment, but also enables a significant reduction in processing equipment and processing costs. The results obtained are expected to contribute to the practical use of glass interposers and multi-package semiconductors in the future.

Acknowledgement

This paper is based on results obtained from “Research and Development Project of the Enhanced Infrastructures for Post-5G Information and Communication Systems” (JPNP20017), subsidized by the New Energy and Industrial Technology Development Organization (NEDO) of Japan.

References

[1] A. Usman, E. Shah, N. B. Satishprasad, J. Chen, S. A. Bohlemann, S. H. Shami, A. A. Eftekhar, and A. Adibi: IEEE Trans. Compon. Package. Manuf. Technol., 7, (2017) 819.

[2] J. Ihlemann, B. Wolff-Rottke: Appl. Surf. Sci., 106, (1996) 282

[3] R. Karstens, A. Gödecke, A. Prießner, and J. Ihlemann: Opt. Laser Technol., 83, (2016) 16

[4] J. Ihlemann, B. Wolff, and P. Simon, Appl. Phys. A, 54, (1992) 263

[5] E. Terasawa, T. Shibuya, D. Satoh, Y. Moriai, H. Ogawa, M. Tanaka, R. Kuroda, K. Sakaue, and M. Washio: Appl. Phys. A, 126, (2020) 446.

[6] K. Goya, T. Itoha, A. Seki, and K. Watanabe: Sens. and Actuators B: Chem., 210, (2015) 685.

[7] D. Franz, T. Häfner, T. Kunz, G. Roth, S. Rung, C. Esen, and R. Franz: Mater. 15, (2022) 3932.

[8] Y. Ito, R. Shinomoto, K. Nagato, A. Otsu, K. Tatsukoshi, Y. Fukasawa, T. Kizaki, N. Sugita, and M. Mitsuishi: Appl. Phys. A, 124, (2018) 181.

[9] M. Kobayashi, K. Kakizaki, H. Oizumi, T. Mimura, J. Fujimoto, and H. Mizoguchi: Proc. SPIE, Vol. 10238, (2017) 10238D.

[10] Y. Kawasuji, Y. Adachi, K. Moro, K. Kakizaki, and M. Washio: J. Laser Micro Nanoeng., 17, (2022) 133.

(Received: May 18, 2023, Accepted: December 11, 2023)